ORIGINAL ARTICLE

Development of Hot Wire GTAW Process for 18% Ni Maraging Steel Used for Rocket Motor Casing

Chidanand Magadum[1] · P. Senthil[1] · M. Manohar[2] ·
S. Biju[2] · Uday Parmar[3] · Rohit Kumar Gupta[2]

Abstract Maraging steels possess ultrahigh strength and excellent fracture toughness which makes it suitable for rocket motor casing and other applications. Though it has good weldability and effectively welded by conventional or cold wire Gas Tungsten Arc Welding (CW-GTAW), defects like entrapped slag, lack of fusion, porosity, etc., are encountered. The weld pool is also sluggish and does not flow freely as with carbon steel or stainless steels and has limitation of low speed and hence lower deposition rates. The hot wire GTAW (HW-GTAW) process is ideally suited for increasing the weld fluidity which helps the slag to afloat easily. It also provides the benefit of elimination of porosity from the weld deposit along with increased weld speed and deposition.

In present work, HW-GTAW process was used to weld 8 mm thick maraging steel to reduce slag formation and other types of defects. Welding was done with higher welding speed and higher wire feed rate resulting in higher deposition. Bead on trials with HW-GTAW were conducted to establish the relation between travel speed, wire feed rate and hot wire current. Transverse tensile properties and fracture toughness of weldments were evaluated. Macro and microstructure analysis of weldment was carried out to analyse the various zones. Microhardness across the weld was measured. UTS of 1720–1749 MPa, 0.2% PS of 1687–1713 MPa and FT upto 89 MPa$\sqrt{m}$ was achieved with joint efficiency between 93 and 90% on tensile and fracture toughness, respectively, using HW-GTAW process. Microstructure of weld fusion zone showed dendritic structure having martensite with narrow dark HAZ containing reverted austenite. Reduction in heat input, minimal defects and improved productivity was achieved by using HW-GTAW process.

1 Introduction

18% Ni maraging steel is a special class of high strength steel, hardened by metallurgical process that does not involve carbon and possess ultrahigh strength combined with excellent toughness. These are strengthened by precipitation of inter-metallic phases, by ageing at 480 °C for 3.5 h. This special characteristic along with easy weldability, has made 18% Ni maraging steel a suitable option in the aerospace industry for the manufacturing of rocket motor casings of launch vehicles.

Although the weldability of maraging steels is very good, attaining the strength and fracture toughness of weldments comparable to base metals is one of the major concerns. A number of studies have indicated superiority of the GTAW process for maraging steels over other fusion welding techniques. Knoth and Lang conducted experimental work with GTAW and GMAW (Gas Metal Arc Welding) and observed much lower fracture toughness (K_{1C}) values for both welds [1]. Submerged arc welding (SAW) of maraging steel has shown loss of Ti and pick-up of Si and Mn in the weld causing very low weld toughness [2]. Lee et al. [3] studied electron beam welding on 1.7 mm thick maraging steel. Though more than 95% weld efficiency with respect to strength was achieved, a significant reduction in

✉ P. Senthil
  senthil@nitt.edu

[1] Department of Production Engineering, National Institute of Technology, Tiruchirappalli, India

[2] Materials and Mechanical Entity, Vikram Sarabhai Space Centre, Thiruvananthapuram, India

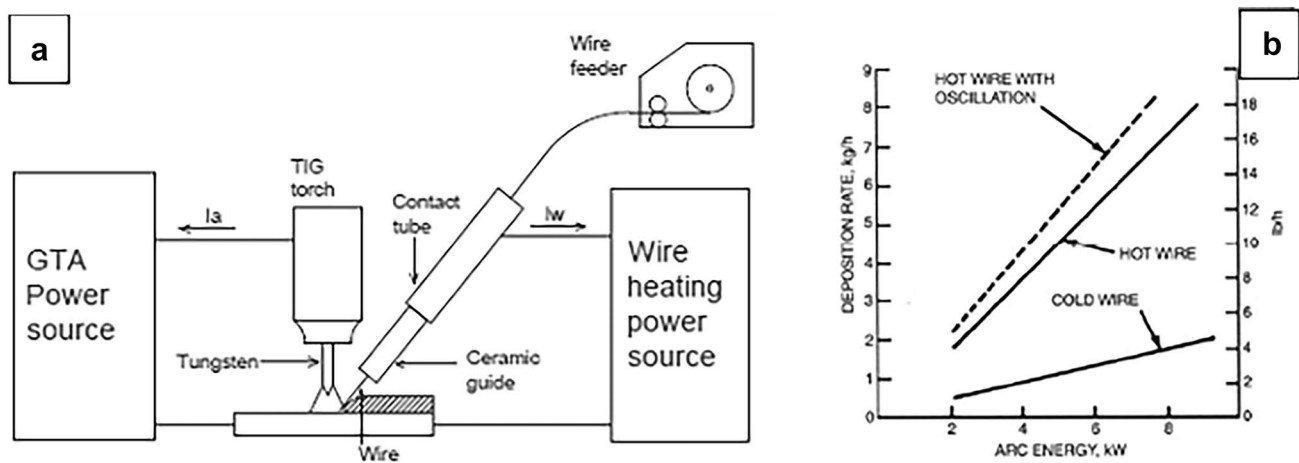[3] Larsen & Toubro Limited, Powai, Mumbai, India

Fig. 1 **a** Schematic of HW-GTAW process, **b** Comparison of deposition rate of CW & HWGTAW

elongation was noted. Subashini et al. [4] reported lower fracture toughness of welds in single pass laser-MIG (Metal Inert gas) hybrid technique. Gupta et al. [5] compared multipass GTAW of 8 mm thick maraging steel with single pass keyhole plasma arc welding (PAW), and found comparable mechanical properties. Meshram et al. [6] evaluated friction stir welding on 5.5 mm thick maraging steel. Being a solid-state welding process, microstructure was found to be free from reverted austenite and showed superior impact toughness. But the selection of the correct FSW tool material for high strength maraging steel is a real challenge [7].

Microstructurally maraging steel weldments contain different zones. Adjacent to the fusion zone is HAZ, which has well-defined zones viz. coarse-grained zone, light etched zone, and dark etched zone [8, 9]. Rohit and Muktinutalapati studied the reversion of austenite in maraging steel weldments. The micro segregation in fusion zone of weld is an important character for the formation of reverted austenite [10]. Also, maraging steel weldments exhibit the phenomenon of delayed cracking, formation of small cracks at the interface of dark HAZ due to peak temperature of weldments resulted by thermal cycling [11]. Several studies reveal that 90–95% of strength and 70–90%of toughness compared to base metal can be achieved in welds depending on variables like heat input and filler metal composition [12].

Fabrication of maraging steel component involves typically 3–15 mm weld thickness. High energy density welding processes are not appropriate for parts designed based on fracture properties [4, 13]. GTAW is an obvious choice for welding of these steel with respect to the strength and the toughness [14]. Currently, industries are using cold wire (CW)-GTAW process to realize maraging steel rocket motor casings. However, it has serious economic limitations because of its low speed and low deposition rates limiting the productivity in several industries. It is seen in weld radiography that the maraging steel weldment encounters slag inclusions issue also. Weld pool in maraging steel is sluggish, which leads to entrapping slag adherents. Recently, Agilan et al. studied the slag formation problem in maraging steel weldments and used activated flux (CaF_2) to eliminate slag [15, 16].

To address these issues, hot wire (HW)-GTAW process is proposed and studied in the present work. The process is ideally suited for increasing the weld fluidity which helps the slag to afloat easily and also provides the benefit of virtual elimination of porosity from the weld deposit, resulting in cleaner and faster weld. The HW-GTAW process is a variant of the CW-GTAW process, in that filler metal is preheated prior to its entry in the weld pool (Fig. 1a). As preheated wire enters the weld pool, nearly all energy of the welding arc is available for penetration or to generate the weld pool and hence chances of lack of fusion (LOF) reduces drastically. Due to resistance heating (I^2R) of the filler metal (as it approaches the weld pool), most of the surface contaminations in the wire are burnt off, which minimizes chance for porosities. With high currents (> 200 A) and HW current of typically 50–80 A, it is easy to maintain adequate weld fluidity. The HW process gives higher deposition rates compared to the CW process as shown in Fig. 1b [17].

In view of the numerous advantages of HW-GTAW process, an attempt is made to study and induct this process in the welding of maraging steel. In this work, main objective is to establish HW-GTAW parameters for maraging steel welding and eliminate/ minimize defects like entrapped slag, porosity and LOF from the weld. Other advantages are reduction in heat input, increase in deposition rate by increasing the weld travel speed, reduction in number of weld passes and increase in productivity. For comparison, CW-GTAW process has also been included in the present work. Transverse tensile and fracture toughness specimen

Table 1 Chemistry of material (in wt. %) used in welding study

Element	C	Mn	Si	Mo	Ni	Co	Ti	Al	O$_2$ (ppm)	H$_2$ (ppm)	N$_2$ (ppm)
Base metal	0.003	0.03	0.01	4.9	18.05	8.12	0.46	0.09	5	1	8
Filler metal	0.006	0.01	0.015	2.58	18.32	11.96	0.17	0.42	34	1.8	8

Table 2 Welding parameters used for CW-GTA welding in 4 passes

Weld Pass	1	2	3	4
Current (A)	225	230	230	240
Voltage (V)	10	12	12	14
Travel Speed(mm/min)	78	95	95	88
Wire feed(mm/min)	620	630	640	700
Heat Input (kJ/mm)	1.73	1.74	1.74	2.29

have been subjected to ageing and mechanical properties of the welds have been determined. Comparison of mechanical properties, macro and microstructure of welds produced by CW and HW has been carried out.

2 Experimental

Initially bead on trials were carried out to find the maximum HW current at which wire can withstand before resistive melting. Bead geometry was studied with wire feed rate of 800, 1000, 1200 and 1400 mm/min at different hot wire current, namely 35 A, 50 A, 65 A, 80 A and 100 A at constant arc current of 240 A. Macrostructure of beads was taken at 10× and bead width, height and depth of penetration were measured.

Further, plates of size 8 mm × 150 mm × 500 mm and filler wire of diameter 1.6 mm were used in the experiment. Filler wire with slight increase in cobalt and aluminum and reduced molybdenum and titanium contents (W2) was used for welding of maraging steel for better weld fracture properties. By lowering Mo and Ti, increase in Co and addition of Al, austenite in weld was reduced ensuring improvement in strength and toughness of weld joint [12]. Chemistry of base metal and filler wire is shown in Table 1. For welding, V-groove weld joint configuration with included angle 60° and root gap 2 mm was used.

One coupon plate was welded with CW GTAW process with 4 passes as per the welding parameters in Table 2. To optimize the weld parameter and to reduce heat input, 3 pass welding trials were conducted in HW GTAW process. To complete the 8 mm thick welding in 3 passes, the variation in the travel speed was done and after each pass welding, remaining depth to fill the groove was measured and parameters were frozen accordingly. Three coupons were welded with HW GTAW process. Welding parameters used in trials along with fixed parameters are given in Tables 3 and 4. Many authors calculated the net heat input in HW GTAW process. It is the sum of main arc heat and auxiliary heat given to the filler wire [18–20]. By changing the HW current (I_h) and wire stick-out length (l), resistance heating of the filler wire can be changed. The auxiliary heat input is very small compared to the main arc heat.

Main Arc heat input = (voltage × current × 60/travel speed) × 1000
Auxiliary heat input = Power × 60/wire feed rate

Power = $I_h^2 R$, where $R = \rho l / A$; ρ = resistivity, 600–700 μΩ mm in annealed condition; l = stick-out length, mm, A = area, mm^2.

Welded coupons were made to undergo nondestructive examinations (NDE), namely dye-penetrant (DP), ultrasonic-test (UT) and X-ray radiography test (RT). Aerospace material specification (AMS) 2632A was used as reference procedure for ultrasonic examination. Angle beam scanning was carried out using 45°, 60° and 70° probes with AMS G-notch as standard reference reflectors. Radiographic examination was conducted with X-ray of less than 2 mm spot size. Sensitivity of the technique is ≤2% of the base metal thickness. Acceptable porosity limit is of diameter 1.2 mm whereas LOF, lack of penetration and undercut are not acceptable. DP test was as per the reference code of ASME Section-V, article 6. Specimens were machined from the weld and ageing treatment was carried out at 485°C for 3.5 h in an electrical resistance furnace. Tensile test

Table 3 Fixed parameters used for HW GTA welding

Tungsten diameter: 4 mm	Distance between HW and electrode: 2–3 mm
Tungsten stick-out: 12-13 mm	Shielding gas flow rate (GFR): 15–20L/min
Filler wire diameter: 1.6 mm	HW wire shielding GFR: 25–30 L/min
HW wire stick-out: 25–30 mm	Trailing GFR: 25–30 L/min
Angle of hot wire torch: 30°	Backing GFR: 10–15 L/min

FGR gas flow rate

Table 4 Welding parameters used for welding in 3 passes

Weld pass	Trial 1			Trial 2			Trial 3		
	1	2	3	1	2	3	1	2	3
Current (A)	215	230	230	215	230	230	215	220	230
Voltage (V)	9.6	12	14	9.6	12	14	11	12	14
Travel Speed (mm/min)	80	88	95	85	90	80	95	100	110
Wire feed (mm/min)	650	720	720	680	720	860	880	950	1200
HW Current (A)	55	55	55	55	55	55	55	60	70
Heat Input (kJ/mm)	1.55	1.88	2.03	1.46	1.84	2.42	1.49	1.58	1.76
Total heat input (kJ/mm)*	1.55	1.88	2.03	1.46	1.84	2.42	1.49	1.58	1.76

*Including auxiliary heat-input ranging from 0.00169 to 0.00223 kJ/mm

(TT) specimens were made and tested as per the standard ASTM-E8 [21]. Rectangular specimen of 12.5 mm width with 50 mm gage length were prepared and tensile testing was carried out with strain rate of 2.5×10^{-4} per second. For fracture toughness test, compact tensile specimens (CTS) were prepared with Chevron type fatigue crack starter notch. Notch was machined at the center of the weld and oriented along the direction of the welding so that during testing, crack propagation was along the weld. Fatigue pre-cracking was produced using 25 Hz cyclic loading with 3.5 kN load and plain strain fracture toughness (K_{1C}) testing was conducted as per ASTM-E399 [22]. Microhardness survey of weld and HAZ was carried out. Weld cross sections were etched by using 5% Nital solution for macro and micro examinations as per standard ASTM-E3. The transverse section of the specimen was prepared by adopting mechanical grinding and polishing techniques. For optical microscopy, Modified Fry's Agent was used as etchant. Tested specimens were examined under scanning electron microscope for fracture surface observation.

3 Results and Discussion
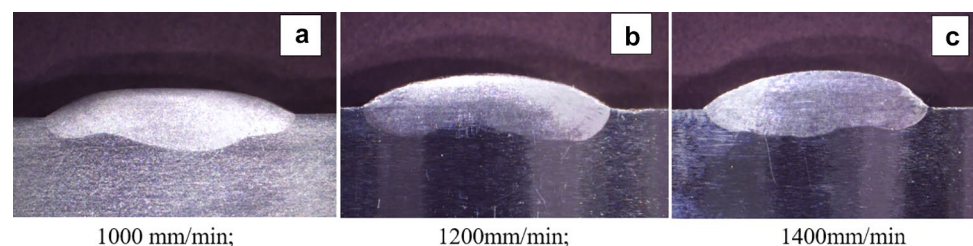
3.1 Bead on Trials

To find out the correlation between HW current and wire feed rate, bead on trials were carried out. It was observed that, if the hot wire current is too high, the wire separates from the weld puddle and melts back, forming a ball on the end of the wire. The resistance heating of the filler wire

varies with wire feed rate for the given value of HW current. For a constant wire feed rate, the hot wire current was varied to find out the weld bead profile. At given hot wire current, there exists a range of wire feed rate in which uninterrupted welding takes place. At higher wire feed rate, push feeding of wire into the arc takes place disturbing main arc. Similarly, at lower wire feed rate, droplet transfer forms resulting in interrupted welding. Hence, optimum wire feed rate at given HW current is required to establish continuous and smooth welding. Macrostructure of the weld bead at different wire feed rate at 50 A HW current is shown in Fig. 2. The effect of variation in the HW current (35–100 A) at different wire feed rate (800, 1000, 1200, 1400 mm/min) on the measured bead width and bead height at constant welding current of 250 A are shown in Fig. 3. At constant wire feed rate, increase in HW current increases the bead width and decreases the bead height. It is noticed that at constant welding current, weld reinforcement improves with the increase in wire feed rate. This is because increase in HW current enhances the resistance heating of filler wire and increases the liquidity of molten pool. This accelerates the weld buildup resulting in sideway displacement of molten liquid and increases the reinforcement width. Similar effect was reported by many authors [18, 19, 23]. Penetration is mainly influenced by the variations in arc heat and little influence on variation in resistance heating of filler metal.

3.2 Plate Welding

One plate coupon was welded with CW-GTAW process as per the parameters mentioned in Table 2. Based on the

Fig. 2 Macrostructure of weld bead at HW current of 50 A at different wire feed **a** 1000 mm/min **b** 1200 mm/min **c** 1400 mm/min
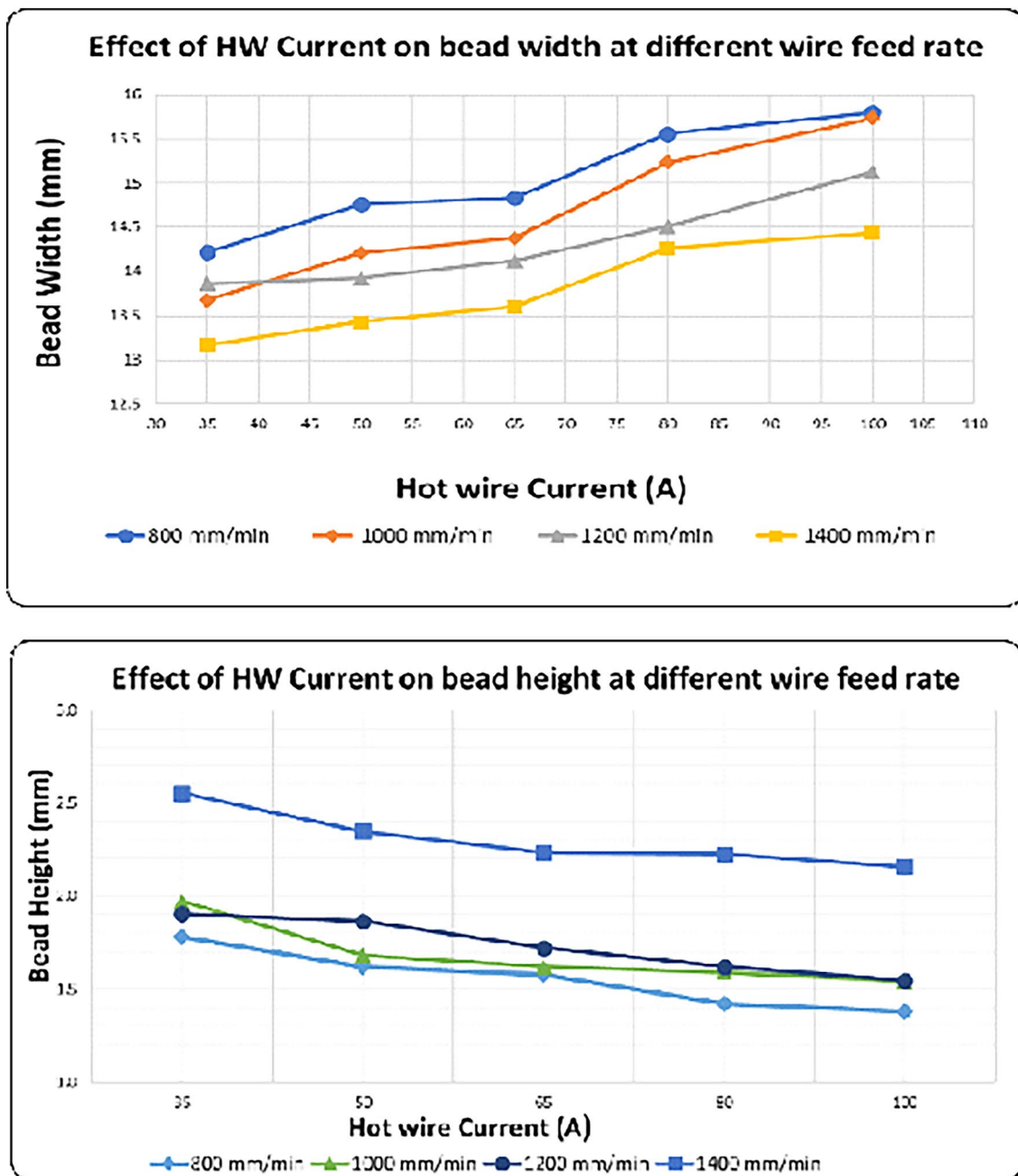
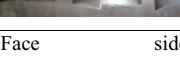1000 mm/min;   1200mm/min;   1400mm/min

Fig. 3 Variation of bead width and height with HW current at different wire feed rate

bead on trials and few initial welding trials, 3 coupons were welded by HW-GTAW process as per the parameters given in Tables 3 and 4 and the outcome is highlighted in Table 5. In trial-1, wire feed and travel speed were optimized and welding was carried out as per the parameters given in Tables 3 and 4. The weld has been found to be visually satisfactory. However, the heat input for the 3rd weld pass is insufficient to cover the balance groove. Under-flush and undercut is observed in the weldment. Moreover, there is LOF. Hence, the plate is rejected and it is not considered for mechanical testing.

During second trial (Table 5), heat input for 3rd pass increases by reducing travel speed from 95 to 80 mm/min. After three pass welding, weld is smoothly merged with the base metal and visually it is found to be free from defects like under-flush and undercuts. No discontinuities open to the surface is indicated by DP. There is no detection of internal defects in RT and UT.

Table 5 Welding bead and NDE observations of weldments

Trials	Weld		NDE
1	Face	side	Under-cut & under-flush observed in Visual and DP
	Root	side	LOF observed in X-Ray
2	Face	side	Weldments found satisfactory in visual, DP, X-ray and UT
	Root	side	Reinforcement not satisfactory
3	Face	side	Weldments found satisfactory in visual, DP, X-ray and UT

It is understood from trial-1 and 2 that optimum parameters shall be used for filling up the groove maintaining low heat input. Although tensile test and fracture toughness results are acceptable (Table 5) in trial-2 welds, 0.2% PS and fracture toughness are low. Fracture toughness of weldment is a direct function of heat input. Lower heat input will lead to under-flush and higher heat input lead to lower mechanical properties. It is noted that the average heat input per pass is 1.91 kJ/mm for trial-2 compared to 1.82 kJ/mm in trial-1. Hence, it is essential to reduce the heat input to improve the 0.2% PS. It is noted that having low heat input in the second pass can narrow down the requirement of heat input in the third pass. This is because, burning of the edges of the V-groove can be prevented in second pass welding and thus the width required to cover the third pass is less, eventually with lower heat input, required reinforcement can be achieved.

In view of the above, trial-3 coupon plate was welded with increased travel speed in both second pass and third pass resulting into heat input of 1.58 and 1.76 kJ/mm, respectively. UTS, 0.2% PS and fracture toughness values are improved with these modified parameters (trial-3 of Table 4). It is noted that around 7% increase in both average UTS and 0.2%PS is observed in trial-3 welds as compared to welds with trial-2. Appreciable increase in fracture properties ($\approx$11%) are observed by reducing the net heat input from 5.72 to 4.83 kJ/mm. Weldments produced with high heat input have been found to fail in the HAZ with reduced joint efficiency because of over aging and higher volume fraction of reverted austenite. High joint efficiencies can be achieved with lower heat input, particularly when welds are age hardened directly after welding.

Less slag formation compared to CW-GTAW is also noticed in HW-GTAW due to wire preheating. This is because heating removes volatile surface contaminants from filler wire. Appearance of the weld bead is excellent along with defect free welds in NDE. It may be noted that the welding was carried out with higher wire feed rate in the order of 1000 mm/min, resulting in higher weld deposition. HW welds are free of distortion and defects. Since welding is completed in 3 passes, arcing time required for completing the weld reduces drastically. Nearly 33% less arcing time is achieved compared with the CW welding process. Higher speed, high deposition rate and lesser weld repairs due to defect free welds lead to higher productivity. Total cycle time reduction in welding for typical rocket motor casing (175 m length) with HW-GTAW process will be around 25% compared to CW-GTAW process.

3.3 Macrostructure and Microstructure Examination

Macrostructure examination was performed in the aged condition on specimen using a stereo microscope to reveal different weld joint regions. The macrograph of HW and CW weld is shown in Fig. 4. It is observed that width of the third pass is less, i.e., 14 mm for weldment welded by hot wire process, which is less than the width obtained for conventional cold wire GTAW (17 mm). This could be due to the lesser number of weld passes in HW, which reduces the edge burning during each pass and restricts the groove opening resulting in narrow width. Figure 4c, d shows the enlarged view of HAZ of HW and CW weldments. Width of the dark band, HAZ-B is comparable with CW and varies between 2.7 mm at top (face) side and 3.4 mm at root side.

Microstructural studies were conducted in aged conditions. Figure 5 shows microstructure of various zones of the weldment. Figure 6 shows the fusion zone of the weld in case of HW and CW weldments after ageing. Weld of the maraging steel has dendritic structure containing martensite and austenite. The austenite phase in the welded zone of maraging steel weldments is identified by its distinct shape (islands) and shiny appearance as shown in Fig. 6. The segregation of alloying elements will be more at the intersection regions of dendrites due to which there will be retained/reverted austenite in these regions upon cooling to room temperature (alloy enrichment lowers Ms temperature and austenite phase is retained). Next to fusion line is characterized by coarse grain martensite. During welding, this region experiences very high temperature resulting in considerable grain growth in the austenitic region. After cooling, the structure converts to coarse martensite. This zone experiences fully austenitic temperature. On cooling the structure transforms to light etched martensite and is denoted as

Fig. 4 Macrostructure of weld and HAZ for HW and CW processed, **a**, **b** weld, **c**, **d** haz
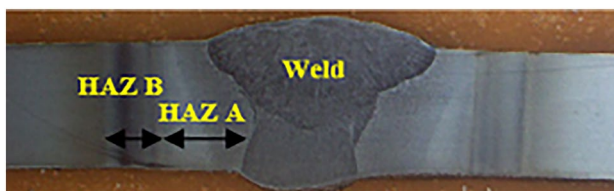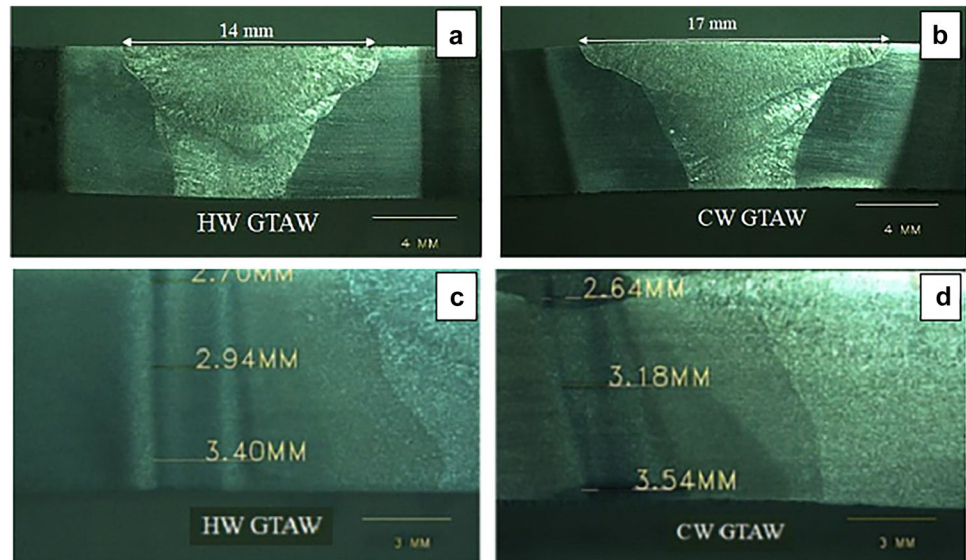

Fig. 5 Microstructure of various zones of weldment representing HW and CW-GTAW process

HAZ-A, as shown in Fig. 7. The dark etch region (HAZ-B) is the region where martensitic phase experiences peak temperatures in the range of 590–730 °C. Some reverted austenite is formed in this region in martensitic matrix due to weld heat. Precipitation is less in such austenite region while ageing which leads to lower hardness as compared to overall weldment. The dark etching region exhibits a two-phase microstructure, where martensite decomposes to alloy depleted martensite and reverted austenite [24]. In this

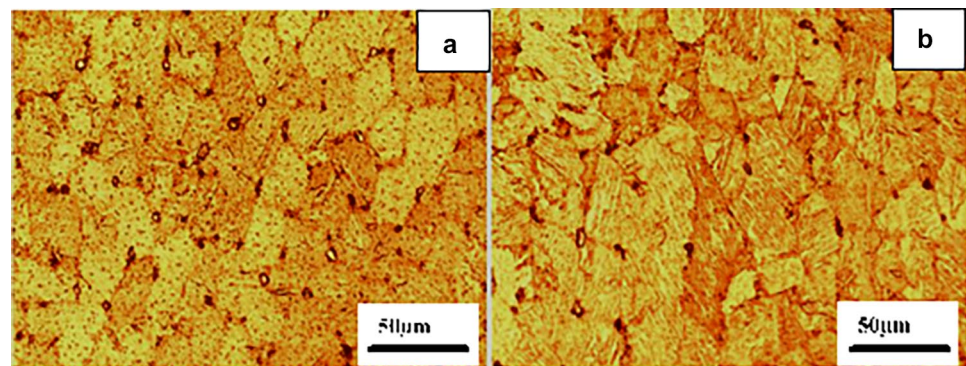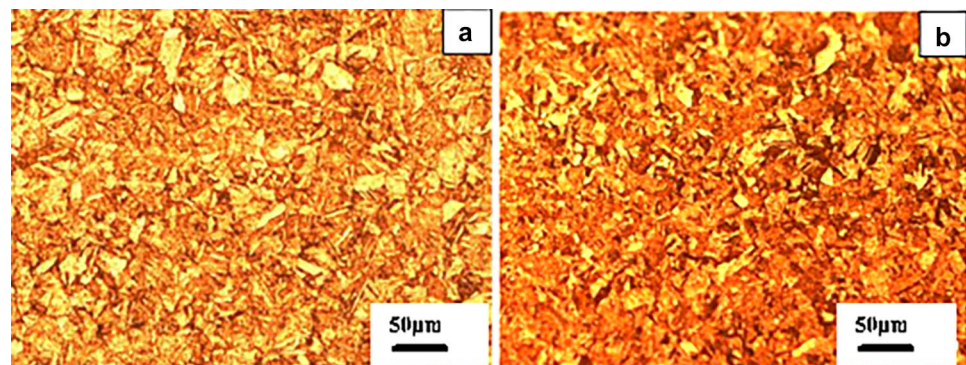Fig. 6 Microstructure of weld in aged condition **a** HW GTAW, **b** CW GTAW

Fig. 7 Microstructure of HAZ-A in aged condition, **a** HW GTAW, **b** CW GTAW

region, reverted austenite is seen in the form of some patches (not in the form of shiny pool). The dark HAZ (HAZ-B) is shown in Fig. 8.

3.4 Chemical Analysis and Microhardness

Chemical analysis (wt.%) of weld at root side shows Ni18.10, Co9.27, Mo3.61, Ti0.362 and top side weld shows Ni18.70, Co10.85, Mo2.87, Ti0.274. More dilution is observed at root side. This is because of single V-joint configuration in which more base metal melts at root side compared to top side. Micro hardness evaluation done in welded and aged condition of weldments at top (face) and bottom (root) of weld is shown in Fig. 9. Higher dilution leads to higher hardness due to availability of alloying elements, namely Mo and Ti, in higher proportion compared to top (face) side which helps in the formation of Ni_3Mo and Ni_3Ti precipitation. It is also evident from the graph shown in Fig. 9b that hardness in the root side is slightly higher than top side. Microhardness variations across the interfaces as a result of welding could be attributed to the welding thermal cycle. In the as welded condition, hardness of the fusion zone is the lowest. Right from the fusion zone, hardness is increasing towards HAZ due to presence of precipitate in this zone during welding. After ageing it is observed that HAZ hardness is lower, as this region exhibits high temperatures during welding, resulting into grain coarsening. HAZ-B region reveals lower hardness due to presence of reverted austenite in this region. These findings are in agreement with earlier investigators [5, 25, 26]. Fusion zone and HAZ hardness are lower than the hardness of base metal in both as welded and as aged condition.

3.5 Tensile and Fracture Properties

The mechanical properties of 18% Ni maraging steel in as received condition (solutionised) is around 950 MPa 0.2% PS and 1050 MPa UTS. As expected, ageing results in a considerable increase in the strength. Table 6 shows the tensile strength and fracture properties of 8 mm thick 18%
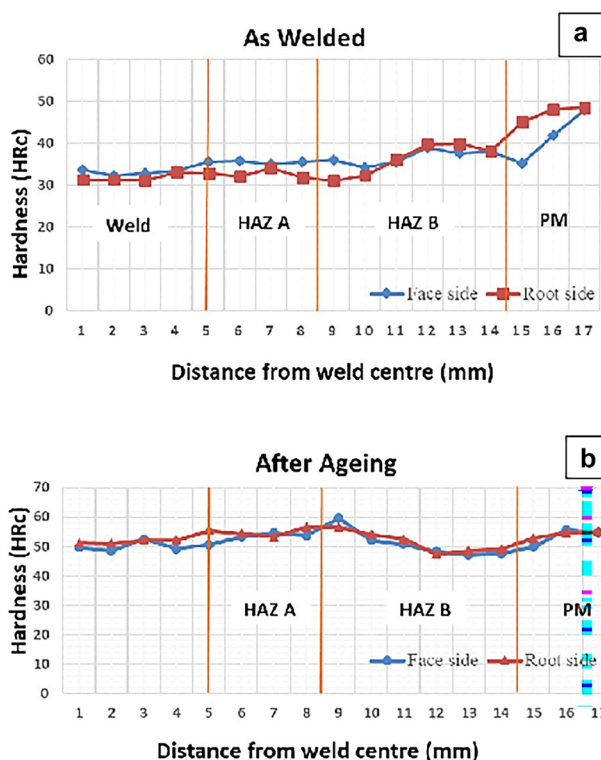
Fig. 9 Micro hardness survey of weldment **a** as welded; **b** after ageing

Ni maraging steel welds produced by CW and HW GTAW process. It is seen that mechanical properties of maraging steel in aged condition are quite satisfactory and comparable with literature data. Also, the properties meet the minimum requirement of 0.2% PS (1550 MPa) for component. Minimum value of 0.2%PS has increased from 1624 to 1687 MPa by using HW GTAW process. The average UTS and 0.2%PS values for welds produced by CW process are 1687 and 1649 MPa, respectively. It is observed that, around 3% increase in weld strength (both UTS and 0.2%PS) is obtained by using HW process in place of CW process. The higher strength of HW welds can be attributed to lower

Fig. 8 Microstructure of HAZ-B in aged condition, **a** HW GTAW, **b** CW GTAW
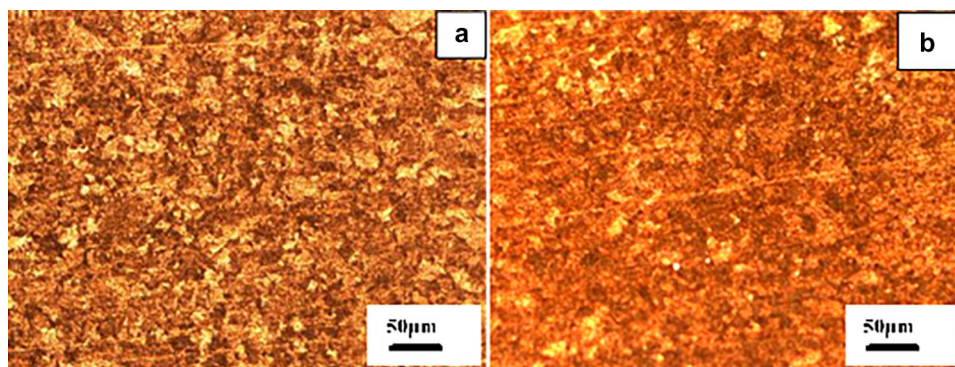
Table 6 Mechanical test results of the samples CW and HW with Trial-2 and 3

	Sample	UTS (MPa)	0.2% PS (MPa)	% Elongation	FT (K_{1C}) MPa$\sqrt{m}$
As solutionised (PM)		1050	900	20	–
Age hardened (PM)		1850	1825	5	95
CW	1	1682	1661	5.35	77.91
	2	1714	1676	5.4	79.32
	3	1702	1658	5.2	80.28
	4	1673	1630	4.8	76.75
	5	1665	1624	4.9	79.73
Trial 2 (HW)	1	1619	1591	5.45	76.54
	2	1624	1582	5.39	77.63
	3	1608	1567	5.6	75.02
Trial 3 (HW)	1	1720	1687	4.40	82.06
	2	1728	1700	5.60	89.78
	3	1737	1691	5.42	86.56
	4	1749	1710	5.65	82.11
	5	1747	1713	6.21	86.35
	6	1747	1706	5.28	84.13

heat input, cleaner welds and elimination of entrapped gases and porosities due to heating of filler wire. Higher heat input leads to prolonged heating at higher temperature resulting in increased amount of reverted austenite. It decreases both UTS and 0.2%PS of weldment [27, 28].

It may be noted that HW GTAW process was carried out with relatively higher speeds (average welding speed of 102 mm/min) with less number of passes (3 pass). As current and voltage are nearly similar in both the welding processes, higher welding speed in HW process results in lower heat input to the welds. The lower tensile strength in CW weld is primarily due to coarser grain structure formed by slow cooling rate as a result of high heat input and secondly due to presence of austenite [14]. Higher heat input governs the cooling rate, grain size and weld bead width. The net heat input in the welds of CW and HW are 7.5 kJ/mm and 4.83 kJ/mm, respectively. It is observed that the fracture toughness values for HW welds are superior than CW welds. Fracture toughness values for HW welds are ranging from 82–89 MPa$\sqrt{m}$ against 77–80 MPa$\sqrt{m}$ for CW welds produced by CW GTAW process. Lower fracture toughness for CW welds is because of broader dark etching zone (HAZ-B) characterized by higher volume fraction of austenite. Toughness depends on the size of over grown precipitates and amount of reverted austenite. Cracks nucleate at these weaker phases of austenite and subsequently propagate resulting in fracture during loading. To get the optimal strength and toughness in maraging steel welds, heat input should be as low as possible but high enough to give defect free welds. Amount of heat input is directly related to number of weld passes used for welding to get sound welds. Though increased number of passes refines the microstructure and improves the mechanical properties, large number of weld passes in maraging steel can cause overaging of bottom layers resulting in reverted austenite. Therefore, it is necessary to balance an optimal range of heat input to get sound weld and optimal strength and toughness. Weld joint efficiency of 93% is achieved for the HW welds with reference to parent metal UTS and 0.2%PS whereas 90% of weld joint efficiency with respect to parent metal fracture toughness.

3.6 Fracture Analysis

Fracture analysis of tested samples were carried out under SEM. Representative fractographs are presented in Fig. 10. It confirms the ductile mode of fracture and is in line with obtained properties of the tested samples as per Table- 6.

4 Conclusions

1. Hot wire (HW) GTAW process has been developed for welding of 8 mm thick 18% Ni maraging steel material. It was found that HW-GTAW process reduces the number of weld passes required from 4 in case of cold wire (CW) GTAW process to 3 and allows to use higher travel speed upto 100 mm/min with a wire feed rate of 1000 mm/min.
2. Effectively the deposition rate is increased and hence the productivity is enhanced by approximately 25% with HW-GTAW process.
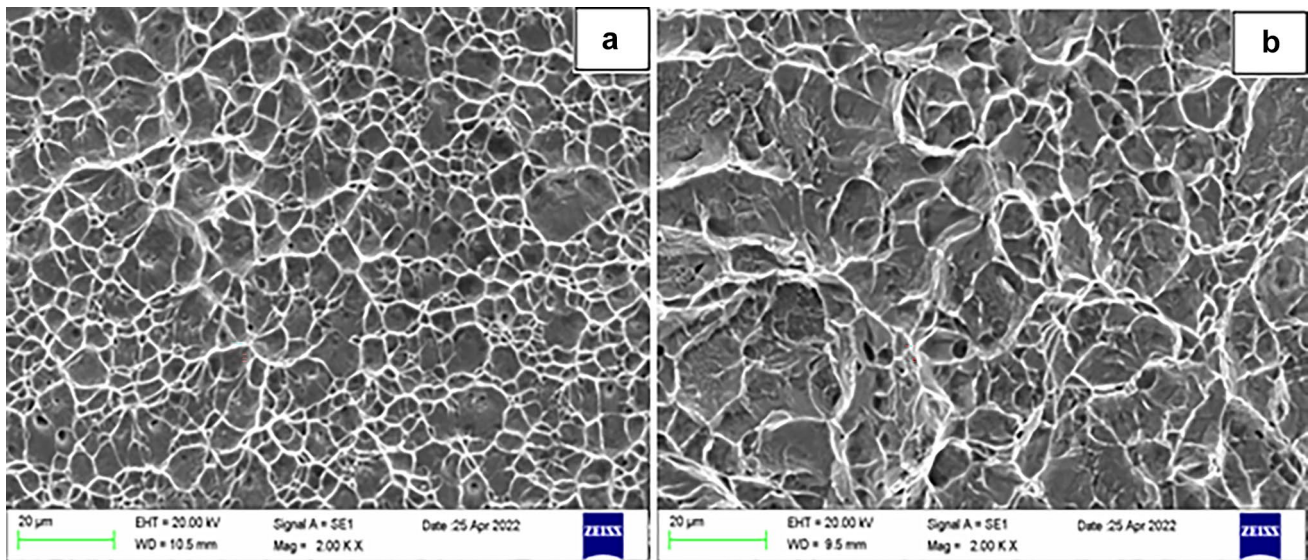
Fig. 10 Representative fractographs of HW welded and tested specimen, **a** tensile tested specimen, **b** fracture toughness tested specimen

3. Improved weld quality is obtained with less slag formation and reduced weld defects like porosity and lack of fusion.

4. UTS of 1720–1749 MPa, 0.2%PS of 1687–1713 MPa and FT upto 89 MPa$\sqrt{}$m has been achieved with HW-GTAW process against UTS of 1665–1714 MPa, 0.2% PS 1624–1676 MPa and fracture toughness upto 80 MPa$\sqrt{}$m are achieved in CW-GTAW process.

5. The weld joint efficiency between 93 and 90% is achieved with 60A of HW current on both tensile and fracture properties.

6. The macrostructure of HW-GTAW weldment reveals that the width of HAZ-B is comparable to CW-GTAW process, i.e., 2.7 mm at top and 3.4 mm at root.

7. Microstructure of weld fusion zone shows dendritic structure with martensite whereas HAZ-B region contains the reverted austenite. Fractography reveals ductile failure on tensile and fracture toughness tested specimens.

References

1. Knoth R J, and Lang F H, *Metals Engineering Quarterly*, **6** (1966) 49.
2. Duffey F D, and Sutar W, *Welding Journal*, **44** (1965) 224.
3. Lee Y J, Lee I K, Wu S C, Kung M C, and Chou P C, *Science and Technology of Welding and Joining*, **7** (2007).
4. Subashini L, Prabhakar K V P, Gundakaram Ravi C, and Padmanabham G, *Materials and Manufacturing Processes*, **31** (2006), 2186.
5. Gupta R, Reddy R, and Mukherjee M K, *Welding in the World*, **56** (2012), 69.
6. Meshram S D, Reddy G M, and Pandey S, *Materials and Design*, **49** (2013), 58.
7. Meshram S D, Reddy G M, and Pandey S, *Advances in Materials and Processing Technologies* (2021). https://doi.org/10.1080/2374068X.2021.1945287
8. Coleman M C, and Jordan M F, *Metals Technology* (1974).
9. Mittal M C, and Ghose B R, *Weld J, Research Supplement* (1989), 457-s.
10. Rohit B, and Muktinutalapati N R, *Materials Science and Technology* (2017). https://doi.org/10.1080/02670836.2017.1407544
11. Gupta R N, Raja V S, *Materials Science & Engineering A* **774** (2020) 138911. https://doi.org/10.1016/j.msea.2020.138911
12. Shamantha C R, Narayanan R, Iyer K J L, Radhakrishnan V M, Seshadri S K, Sundararajan S, and Sundaresan S, *Science and Technology of Welding and Joining,* **5** (5) (2000).
13. Rao V, Madhusudan V, Reddy G, and Singh A K, *Microstrcture and mechanical properties of electron beam maraging steel weldments—role of post weld heat treatment* (Paper presented at Indian Welding Society Seminar, Mumbai, India, 2010).
14. Sinha P P, *Maraging steels* (Published by publications & public relations, ISRO, India, 2012).
15. Agilan M, Karthikeyan M K, Venkateswaran T, Thomas M, Sivakumar D, Ramkumar P, Sankaravelayutham P, and Venkitakrishnan PV, *Materials Today: Proceedings* **5** (2018) 8216
16. Gupta R N, Raja V S, Mukherjee M K, and Narayana Murty S V, *Metallurgical and Materials Transactions A*, **48A** (2017) 4655. https://doi.org/10.1007/s11661-017-4279-3
17. Manz Saenger J F, and Manz A F, *Weld J*, **47** (1968) 386.
18. Dinesh K, Anandvel B, and Devakumaran K, *International Research Journal of Engineering and Technology (IRJET)* (2018).
19. Anantha Padnabhaman M R, Neelakandan B, and Kandasamy D, *Material Research* **20** (2017) 7687. https://doi.org/10.1590/1980-5373-MR-2016-0321
20. Pai A, Sogalad I, Basavarajappa S, and Kumar P, *International Journal of Pressure Vessels and Piping* (2019). https://doi.org/10.1016/j.ijpvp.2018.12.002

21. Standard test method for plane strain fracture toughness of metallic material, ASTM standard E-399–83. ASTM (1983) 488.

22. Standard test methods for tension testing of metallic materials, ASTM standard E8–88, ASTM (1989) 497.

23. Shah P, and Agarwal C, *Journal of Welding and Joining*, **37** (2019) 41. https://doi.org/10.5781/JWJ.2019.37.2.7

24. Vasudevan V K, Kim S J, and Wayman C M, *Metallurgical Transactions A*, **21A** (1990) 2655.

25. Ahmad B, Tariq F, Baloch RA, and Naz N, *Journal of Materials Engineering and Performance*, **264** (2010) **264**.

26. Gope D K, Kumar P, Chattopadhyaya S, Wuriti G, and Thomas T, *Materials Science and Engineering*, **1104** (2021) 012014. https://doi.org/10.1088/1757-899X/1104/1/012014.

27. Carter C S, *Metallurgical Transactions*, **2** (1971) 1621.

28. Sinha P P, Arumugham S, and Nagarajan K V, *Welding Journal*, **72** (1993) 391-s.